JOURNAL OF COMPUTATIONAL PHYSICS 65, 215–226 (1986)

Guiding Center Magnetostatic Particle Simulation Model in Three Dimensions

S. Y. KIM AND H. OKUDA

Plasma Physics Laboratory, Princeton University, P.O. Box 451, Princeton, New Jersey, 08544

Received May 23, 1985; revised December 3, 1985

A magnetostatic particle simulation model has been developed and tested for a low β plasma in a strong magnetic field. The model makes use of a three-dimensional grid elongated in the direction of a magnetic field in order to simulate plasma waves propagating nearly perpendicular to the magnetic field. Linear interpolation is used for a two-dimensional grid perpendicular to a magnetic field while cubic interpolation is used for the direction of the magnetic field. Full particle dynamics has been used for the motion of ions, while the guiding center approximation has been used for the motion of electrons. It is found that energy conservation is good and the fluctuation spectra of the electric and magnetic fields from the simulation agree with theoretical predictions quite well.

I. INTRODUCTION

Particle simulation of plasmas has been a well-established means of plasma research along with the development of large scale supercomputers. It is playing an important role in comprehension of the inherent and complicated nonlinear processes involved in plasma dynamics [1]. Particle simulation models are extremely useful and desirable in simulation of kinetic processes in magnetically confined plasmas, and in particular, nonlinear behavior of plasma microinstabilities, plasma diffusion, and plasma turbulence have been studied [2, 3].

Full three-dimensional models for both electrostatic and magnetostatic problems have been developed to understand the physical processes mentioned above [4–6]. Such models have been constructed for both cylindrical and toroidal systems using either a two-dimensional grid for the plasma cross section and eigenfunction techniques in the direction of an ambient magnetic field [4, 5] or a full three-dimensional grid elongated in the direction of the external magnetic field [6]. In particular, both electrostatic and magnetostatic models in cylindrical geometry using a three-dimensional grid have been tested for a plasma near thermal equilibrium [6]. In this model a grid elongated in the direction of the magnetic field compared with the two-dimensional grid in the cross section has been used. Thus, the higher interpolations, such as quadratic or cubic splines, are used for the axial direction. For

0021-9991/86 $3.00

the plasma cross section, linear interpolation is used. Full particle dynamics has been used for both ions and electrons.

Instead of treating the full dynamics of electrons, the guiding center approximation along with the predictor–corrector method can be used for the low frequency, $\omega \ll \omega_{ce}$, and long perpendicular wavelength, $k_\perp \rho_e \ll 1$, regimes, where ω_{ce} is the electron gyrofrequency and ρ_e is the electron gyroradius. Such a model has given satisfactory results for the electrostatic simulation in which low frequency particle motion across a magnetic field has been studied [7]. Furthermore, one can use a larger time step in the guiding center model compared with that in the model using full particle dynamics for the motion of electrons.

In this paper, we develop a magnetostatic model using a three-dimensional grid and guiding center approximation for electrons, and test this model for a plasma near thermal equilibrium. As mentioned above, we use a higher order interpolation such as cubic spline for the axial direction and a linear interpolation for the perpendicular direction to a magnetic field. In Section 2, a magnetostatic model, the so-called Darwin model, which is appropriate for the description of a low β ($\beta \equiv$ plasma pressure/magnetic pressure) plasma, is given. The resulting fluctuation spectra of electric and magnetic fields are compared with theoretical predictions in Section 3. Finally, discussions and conclusions are given in Section 4.

II. MAGNETOSTATIC MODEL FOR A LOW β PLASMA

Many of the collective effects in plasmas, fusion or space, are nonrelativistic and nonradiative. The radiation can be excluded when it is not of physical importance. There are many situations, however, in nature and laboratory experiments in which only the low frequency electromagnetic fields are important so that the high frequency radiative fields due to photons may be discarded. Physically the radiative fields do not couple directly to plasma particle motion because of its large phase velocity. We can save considerable computing time if the high frequency radiation fields are separated from the low frequency electromagnetic fields.

A magnetostatic model or Darwin model achieves this goal by eliminating the transverse part of the displacement current in Ampere's law which is responsible for the high frequency radiations [8–10].

We decompose the electromagnetic fields and current density into two components, transverse (T) and longitudinal (L). Then the equations for the electromagnetic fields may be given by

$$\nabla \times \mathbf{B} = \frac{4\pi}{c} \mathbf{J}^{\mathrm{T}} \tag{1a}$$

$$\nabla \times \mathbf{E}^{\mathrm{T}} = -\frac{1}{c}\frac{\partial}{\partial t}\mathbf{B} \tag{1b}$$

$$\nabla^2 \phi = -4\pi\rho; \qquad \mathbf{E}^{\mathrm{L}} = -\nabla\phi. \tag{1c}$$

Note that the term $\partial \mathbf{E}^{\mathrm{T}}/\partial t$ in Eq. (1b) is discarded. This is the only assumption of this retardationless model. The set of equations (1) is combined with

$$\nabla \times \mathbf{E}^{\mathrm{L}} = 0 \tag{2a}$$

$$\nabla \cdot \mathbf{B} = 0 \tag{2b}$$

$$4\pi \mathbf{J}^{\mathrm{L}} + \frac{\partial \mathbf{E}^{\mathrm{L}}}{\partial t} = 0 \tag{2c}$$

where Eqs. (2a) and (2b) indicate the definitions of longitudinal and transverse components, and Eq. (2c) is an expression of conservation of charge.

We consider a simulation model with the set of above equations in a three-dimensional rectangular box in a strong, uniform external magnetic field which is in

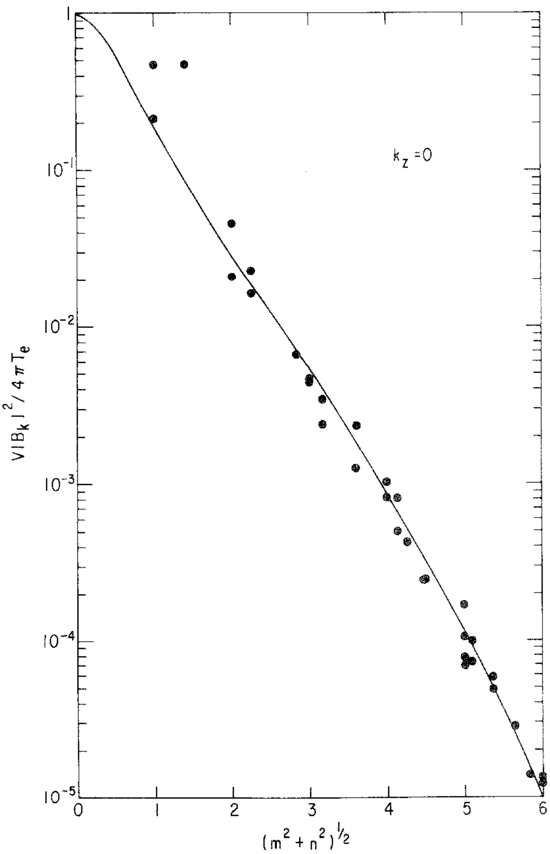

FIG. 1. Time averaged magnetic field fluctuations for the two-dimensional modes, $\mathbf{k} = (k_x, k_y, 0)$, averaged over the entire length of the run. $\omega_{pe} t = 0$–1026 (case 1). The solid line is the theoretical prediction from Eq. (7).

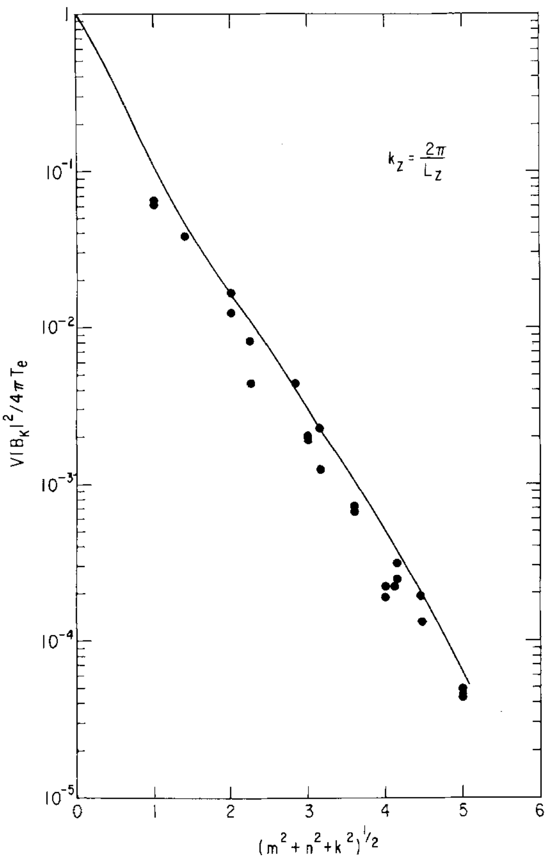

FIG. 2. Time averaged magnetic field fluctuations for the three-dimensional modes, $\mathbf{k} = (k_x, k_y, k_z = \pm 2\pi/L_z)$, averaged over the entire length of the run (case 1). The solid line is the theoretical prediction from Eq. (7).

the z direction. We consider a plasma model elongated along the magnetic field so that $L_z \gg L_x, L_y$, where L_x, L_y, and L_z are the lengths of the simulation plasma in three dimensions. Since $L_z \gg L_x, L_y$, the grid size in z will be much larger than those in x and y. For the cases of low frequency plasma turbulence where modes with $k_\perp \gg k_\parallel$ play an important role, it is enough to keep a few long wavelength modes along the external magnetic field. The short wavelength modes along the magnetic field are heavily damped and are not important.

In the previous model [6], we use full particle dynamics in three dimensions for both ions and electrons. However, when we consider low frequency phenomena, $\omega \ll \omega_{ce}$, the guiding center approximation across the magnetic field can be used for electrons, while the full three-dimensional dynamics is used for ions. This approximation can reduce computing time substantially.

Using Eqs. (1) and the configurations mentioned above, only the x, y components of the self-consistent magnetic field, B_x, B_y, the z component of the transverse electric field, E_z^T, and the full component of the longitudinal electric field, $\mathbf{E}^L$, are calculated, where we assume that $B_z \ll B_0$ and B_z is discarded for a low β plasma [6].

Taking the curl of Eq. (1a),

$$\nabla^2 \mathbf{B} = -\frac{4\pi}{c} \nabla \times \mathbf{J} \tag{3}$$

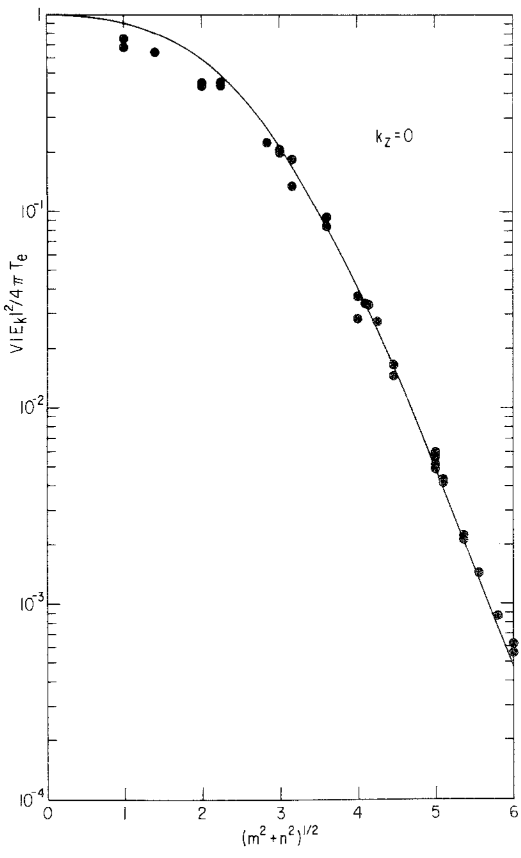

FIG. 3. Time averaged electric field fluctuations for the two-dimensional modes, $\mathbf{k} = (k_x, k_y, 0)$, averaged over the entire length of the run (case 1). The solid line is the theoretical prediction from Eq. (8).

or, in k space,

$$B_x(\mathbf{k}) = i\frac{4\pi}{ck^2}(k_y J_z - k_z J_y) \approx i\frac{4\pi}{ck^2}k_y J_z$$
$$B_y(\mathbf{k}) = i\frac{4\pi}{ck^2}(k_z J_x - k_x J_z) \approx -i\frac{4\pi}{ck^2}k_x J_z \tag{4}$$

where only the z component of $\mathbf{J}$ is retained because $k_z \ll k_\perp$.

For E_Z^{T}, taking the curl of Eq. (1b), we get

$$\nabla^2 \mathbf{E}^{\mathrm{T}} = \frac{4\pi}{c^2}\frac{\partial \mathbf{J}}{\partial t}\bigg|^{\mathrm{T}}$$

or, in k space,

$$-k^2 E_z^{\mathrm{T}} = \frac{4\pi}{c^2}\frac{\partial J_z^{\mathrm{T}}}{\partial t} \tag{5}$$

where E_z^{T} and J_z^{T} are the z components of the transverse electric field $\mathbf{E}^{\mathrm{T}}$ and current density $\mathbf{J}^{\mathrm{T}}$. $\partial\mathbf{J}/\partial t$ is now expressed by using the equation of motion in the guiding center limit,

$$\frac{\partial \mathbf{J}}{\partial t} = -\sum_j e\left[\frac{\partial \mathbf{V}_j}{\partial t} f(\mathbf{r}-\mathbf{r}_j) - \mathbf{v}_j(\mathbf{v}_j\cdot\nabla) f(\mathbf{r}-\mathbf{r}_j)\right]$$
$$= \sum_j \left[\frac{e^2}{m_e}\mathbf{E}_\parallel f(\mathbf{r}-\mathbf{r}_j) + e\mathbf{v}_j(\mathbf{v}_j\cdot\nabla) f(\mathbf{r}-\mathbf{r}_j)\right] \tag{6}$$

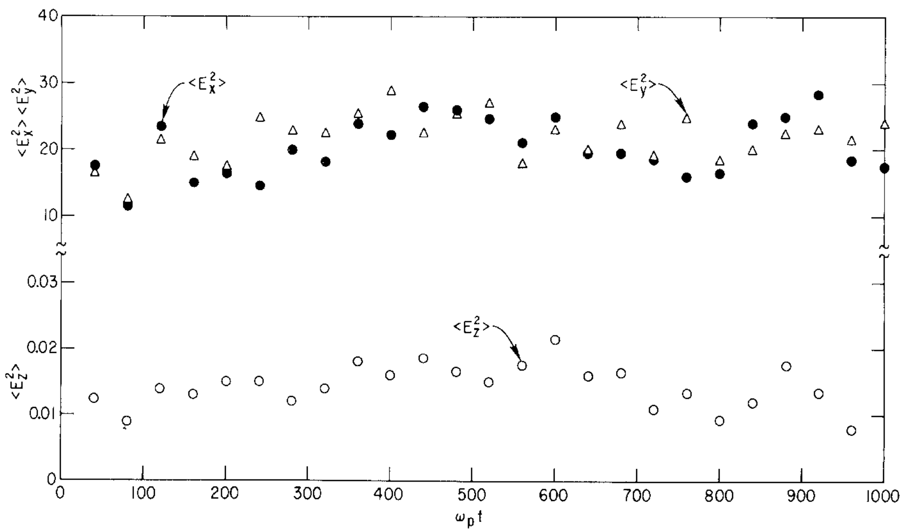

FIG. 4. Temporal behavior of the electric field fluctuations along and across the magnetic field (case 1).

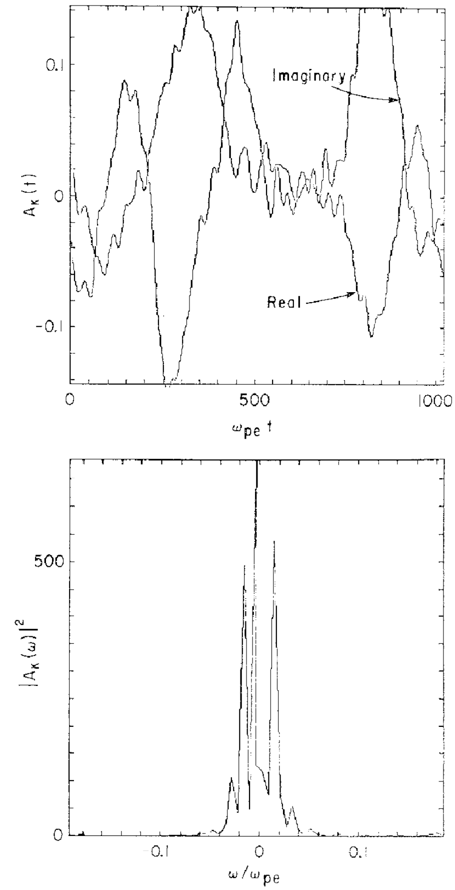

FIG. 5. Time history of the real and imaginary parts of the vector potential, $A_k(t)$, and its frequency spectrum for $(1, 0, 1)$ mode (case 1).

where we assume that most of currents are produced by the electrons. $E_\parallel$ is given by

$$E_\parallel = \frac{\mathbf{E}\cdot\mathbf{B}}{B} = \frac{E_x B_x + E_y B_y + E_z B_z}{B} \simeq E_z + E_x^{\mathrm{L}} \frac{B_x}{B} + E_y^{\mathrm{L}} \frac{B_y}{B}$$

so that

$$\frac{\partial \mathbf{J}}{\partial t} = \sum_j \left[\frac{e^2}{m_e} \left(E_z + E_x^{\mathrm{L}} \frac{B_x}{B} + E_y^{\mathrm{L}} \frac{B_y}{B} \right) \frac{\mathbf{B}}{B} f(\mathbf{r}-\mathbf{r}_j) + e\mathbf{v}_j(\mathbf{v}_j\cdot\nabla) f(\mathbf{r}-\mathbf{r}_j) \right]$$

$$= \sum_j \frac{e^2}{m_e} E_z^{\mathrm{T}} f(\mathbf{r}-\mathbf{r}_j)\,\hat{z} + \mathbf{S} \tag{7}$$

where

$$\mathbf{S}=\sum_j \left[\frac{e^2}{m_e}\left(E_z^L+E_x^L\frac{B_x}{B}+E_y^L\frac{B_y}{B}\right)\frac{\mathbf{B}}{B}f(\mathbf{r}-\mathbf{r}_j)+e\mathbf{v}_j(\mathbf{v}_j\cdot\nabla)f(\mathbf{r}-\mathbf{r}_j)\right]$$

and

$$\mathbf{v}_j=v_\parallel\frac{\mathbf{B}}{B}+c\frac{\mathbf{E}^L\times\mathbf{B}}{B^2}.$$

Substituting Eq. (7) into Eq. (5), we find

$$-k^2E_z^T-\frac{4\pi e^2}{m_e c^2}(nE_z^T)=S_z^T. \tag{8}$$

Equation (8) is solved iteratively as before [6].

III. Test of the Model

The first example concerned (case 1) is the following: $16\times16\times8$ grid in (x, y, z), $16\times16\times640$ Debye length system in (x, y, z), $a_x/\Delta x=a_y/\Delta y=a_z/\Delta z=1$, where a_x, a_y, a_z are the widths of Gaussian particles used, Δx, Δy, Δz are the grid sizes, $m_i/m_e=25$, $T_e/T_i=1$, $\omega_{ce}/\omega_{pe}=2$, $\omega_{pe}\,\Delta t=1$, and total number of particles $=2048$. The system is triply periodic and the plasma is uniform over the entire system. Note that the grid size in z is 80 times larger than Δx and Δy.

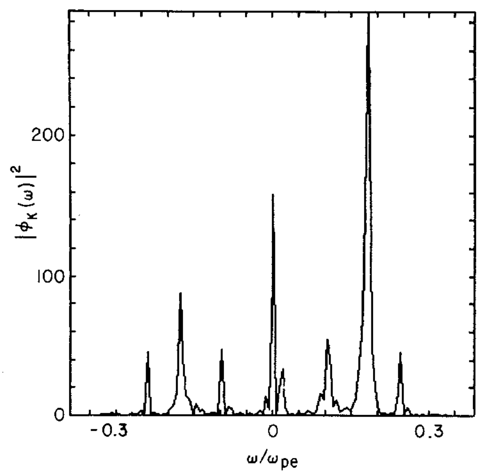

FIG. 6. Frequency spectrum of the electrostatic potential, $\phi_k(t)$ for (1, 0, 1) mode (case 1).

Using a conventional method such as the fast Fourier transform technique, we calculate electric and magnetic fields on the grid points. As a method of charge and force sharing on the grid points, we use linear interpolation in the x–y directions and cubic splines in the z directions. Using a similar time stepping scheme developed by Pritchett and others [9], we calculate the instantaneous values of electric and magnetic fields. After the self-consistent electromagnetic fields are obtained, we push both ions and electrons.

Figures 1 and 2 show the time averaged magnetic field fluctuations for the two-dimensional ($k_z = 0$) and three-dimensional modes ($k_z = \pm 2\pi/L_z$). The theoretical spectrum is given by [6, 11]

$$\frac{V\,|B_k|^2}{8\pi} = \frac{T}{2}\,\frac{1}{1 + (k^2c^2/\omega_{\mathrm{pe}}^2)\,f^{-2}(k)} \tag{7}$$

where

$$f^{-2}(k) = \exp(k_x^2a_x^2 + k_y^2a_y^2 + k_z^2a_z^2)\left(\frac{k_x\,\Delta x/2}{\sin(k_x\,\Delta x/2)}\right)^4\left(\frac{k_y\,\Delta y/2}{\sin(k_y\,\Delta y/2)}\right)^4 \times\left(\frac{k_z\,\Delta z/2}{\sin(k_z\,\Delta z/2)}\right)^8.$$

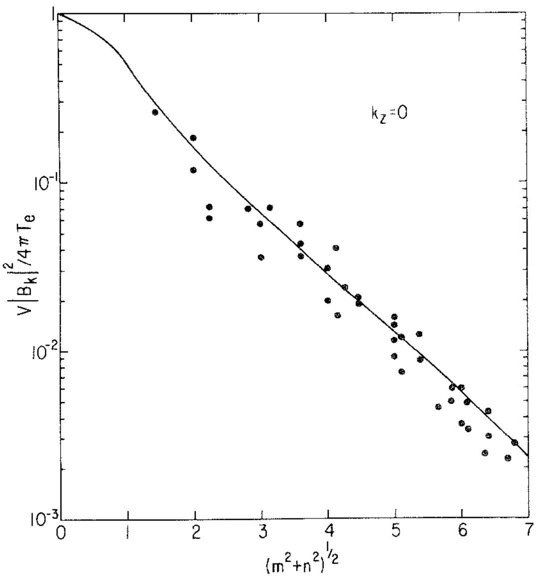

FIG. 7. Time averaged magnetic field fluctuations for the two-dimensional modes, $\mathbf{k} = (k_x, k_y, 0)$, averaged over the entire length of the run. $\omega_{\mathrm{pe}}t = 0$–$2050$ (case 2). The solid line is the theoretical prediction from Eq. (7).

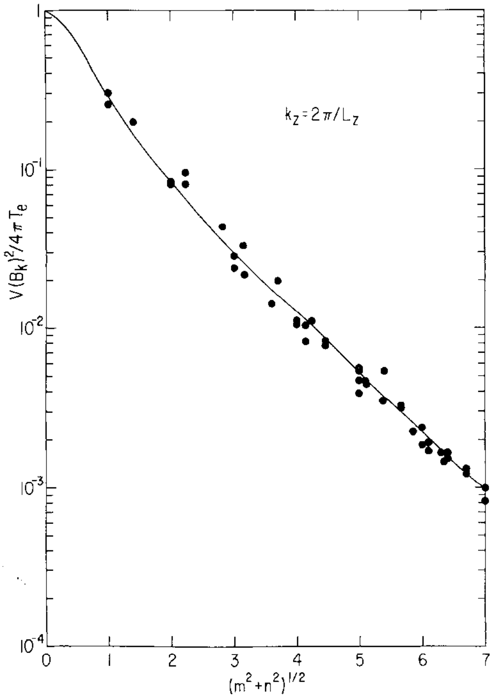

FIG. 8. Time averaged magnetic field fluctuations for the three-dimensional modes, $\mathbf{k} = (k_x, k_y, k_z = \pm 2\pi/L_z)$, averaged over the entire length of the run (case 2). The solid line is the theoretical prediction from Eq. (7).

$f(k)$ is the effective form factor for the linear and cubic interpolations used in the simulation and V is the plasma volume.

Field fluctuation spectra reveal that theory and simulation agree quite well for both zero frequency two-dimensional and three-dimensional shear Alfvén modes. Note that the compressional Alfvén modes do not exist in this spectrum because B_z, the parallel component of B to unperturbed magnetic field B_0, is totally discarded in the low β approximation as discussed in the model.

For electric field fluctuation the theoretical fluctuation is expressed by [6, 11]

$$\frac{V\,|E_k|^2}{8\pi} = \frac{T_e}{2}\,\frac{1}{1 + k^2\lambda_D^2 f^{-2}(k)}. \tag{8}$$

Again both experiment and theory agree very well as shown in Fig. 3. The total energy conservation is about 0.04% at the end of the run (513 steps). Note that the plasma β is 4% here. Temporal behavior of the longitudinal electric field energies in three directions is shown in Fig. 4. There is no apparent sign of growth and they oscillate around the mean value. Note that $\langle E_z^2 \rangle \ll \langle E_z^2 \rangle$ and $\langle E_y^2 \rangle$ because $L_z \gg L_x$ and L_y.

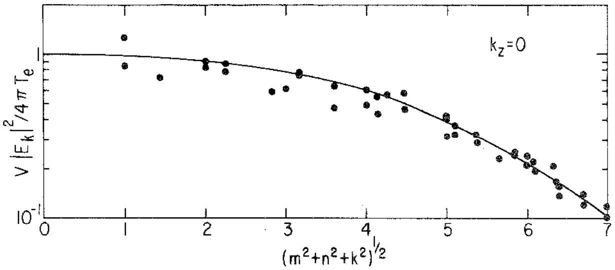

FIG. 9. Time averaged electric field fluctuations for the two-dimensional modes, $\mathbf{k}=(k_x, k_y, 0)$, averaged over the entire length of the run (case 2). The solid line is the theoretical prediction from Eq. (8).

The time history of the real and imaginary parts and the frequency spectrum of the magnetic vector potential for the mode ($m=1$, $n=0$, $k=1$) are shown in Fig. 5. A shear Alfvén wave above the Alfvén frequency, $\omega=k_\parallel v_A$, is found in addition to the peak near $\omega=0$ which is zero frequency magnetostatic mode. The frequency spectrum of the electrostatic potential for the mode ($m=1$, $n=0$, $k=1$) is shown in Fig. 6. Ion Bernstein waves above the harmonics at the ion gyrofrequency, $\omega \simeq n\omega_{ci}$, are found in addition to the small low frequency peaks at the Alfvén frequency, $\omega=kv_A$. The peak near $\omega \simeq 0$ is the low frequency ion acoustic wave near $\omega=k_\parallel c_s$, which is heavily damped in an isothermal plasma ($T_e \simeq T_i$) due to ion Landau damping.

The second example (case 2) has more grids in the x and y directions than in case 1. The parameters are the following: $32 \times 32 \times 8$ grid in (x, y, z), $32 \times 32 \times 640$ Debye length system in (x, y, z), and total number of particles $=8192$. The rest of the simulation parameters are exactly the same as those used in case 1. Figures 7 and 8 show the time averaged magnetic fluctuations for $k_z=0$ and three-dimensional modes for $k_z=2\pi/L_z$. Both results agree quite well with the theoretical spectrum. The comparison between measurement and theory of electric field fluctuation is shown in Fig. 9. Again the simulation result is consistent with the theory. Note that the energy conservation is about 0.02% at the end of the run.

IV. DISCUSSIONS AND CONCLUSIONS

We have developed magnetostatic particle simulation models in three dimensions using the guiding center approximation for electrons. In this model a three-dimensional spatial grid elongated along the magnetic field was used. Linear interpolation was used for the plasma cross section while cubic interpolation was used along the magnetic field.

Near thermal equilibrium both theoretical prediction and measurement agree quite well for both magnetic and electric field fluctuation. During the computing run conservation of energy is extremely good. The code developed here may be useful for both space and laboratory plasma simulations. Drift Alfvén instability in a magnetic confinement device or generation and propagation of Alfvén waves in the magnetosphere are some examples.

ACKNOWLEDGMENTS

This work was supported by National Science Foundation Grant ATM 85-12512 and U.S. Department of Energy Contract DE-AC02-76-CHO-3073.

REFERENCES

1. C. K. BIRDSALL AND A. B. LANGDON, *Plasma Physics via Computer Simulation* (McGraw–Hill, New York, 1985), p. 55.
2. C. K. BIRDSALL, A. B. LANGDON, AND H. OKUDA, "Finite-Size Particle Physics applied to Plasma Simulation," *Methods in Computational Physics*, edited by B. Alder (Academic Press, New York, 1970), Vol. 9, p. 241.
3. J. M. DAWSON, H. OKUDA, AND B. ROSEN, "Collective Transport in Plasmas," *Methods in Computational Physics*, edited by J. Killeen (Academic Press, New York, 1976), Vol. 16, p. 282.
4. C. Z. CHENG AND H. OKUDA, *Phys. Rev. Lett.* **38**, 308 (1977).
5. C. Z. CHENG AND H. OKUDA, *J. Comput. Phys.* **25**, 133 (1977).
6. H. OKUDA, W. W. LEE, AND C. Z. CHENG, *Comput. Phys. Commun.* **17**, 233 (1979).
7. W. W. LEE AND H. OKUDA, *J. Comput. Phys.* **26**, 139 (1978).
8. A. HASEGAWA AND H. OKUDA, *Phys. Fluids* **11**, 1995 (1968).
9. J. BUSNARDO-NETO, P. L. PRITCHETT, A. T. LIN, AND J. M. DAWSON, *J. Comput. Phys.* **23**, 300 (1977).
10. C. W. NIELSON AND H. R. LEWIS, "Particle-Code Models in the Nonradiative Limit," *Methods in Computational Physics*, edited by J. Killeen (Academic Press, New York, 1976), Vol. 16, p. 367.
11. J. M. DAWSON, *Rev. Mod. Phys.* **55**, 453 (1983).